Available online at www.sciencedirect.com
ScienceDirect
Journal of Photochemistry and Photobiology A: Chemistry 182 (2006) 245–249
Journal of Photochemistry and Photobiology A:Chemistry
www.elsevier.com/locate/jphotochem

Correlation of molecular structure, packing motif and thin-film transistor characteristics of solution-processed n-type organic semiconductors based on dodecyl-substituted C_{60} derivatives

Masayuki Chikamatsu [a,*], Atsushi Itakura [a], Yuji Yoshida [a], Reiko Azumi [a,*], Koichi Kikuchi [b], Kiyoshi Yase [a]

[a] *Photonics Research Institute, National Institute of Advanced Industrial Science and Technology (AIST), Central 5, 1-1-1 Higashi, Tsukuba, Ibaraki 305-8565, Japan*
[b] *Department of Chemistry, Tokyo Metropolitan University, Hachioji, Tokyo 192-0397, Japan*

Available online 14 July 2006

Abstract

We report the performance of solution-processed n-type organic thin-film transistors (OTFTs) based on four different types of dodecyl-substituted C_{60} derivatives. Crystallinity and morphology of the spin-coated films highly depend on the compounds. C60-fused *N*-methylpyrrolidine-*meta*-C12 phenyl (C60MC12) exhibited the highest crystallinity and mobility of 0.09 cm^2/Vs among the compounds investigated. We found that not only chain-length but also chain-orientation play an important role for fabrication of highly ordered crystalline film, leading to high electron mobility in solution-processed n-type OTFTs.

Keywords: n-Type organic semiconductor; Fullerene; Solution-process; Organic thin-film transistor; Field-effect electron mobility

1. Introduction

Solution-processed organic thin-film transistors (OTFTs) have attracted considerable interest in resent years for their potential application to low-cost and large-area flexible electronics, such as active-matrix displays and radiofrequency identification [1,2]. A number of promising solution-processed p-type OTFTs have been reported such as polythiophenes [3–6], oligothiophenes [7,8], pentacenes [9–11] and functionalized acenes [12]. However, there have been only several reports concerning solution-processed n-type OTFTs with high electron mobility [13–16]. High-performance n-type materials are needed for realization of printable organic complementary metal-oxide semiconductor circuit, which requires both p- and n-type materials.

Recently, it has been reported that solution-processable C_{60}, [6,6]-phenyl C61-butyric acid methyl ester (PCBM), shows high field-effect electron mobility [14,15]. However, the spin-coated PCBM film takes a disordered structure [17]. Aiming at higher mobility of solution-processable C_{60}-TFT by improving the molecular order in the film, we have focused on long chain alkyl-substituted C_{60} [18,19]. Advantage of this compound is not only high solubility for organic solvent but also easy fabrication of highly ordered films by using self-assembling ability of long alkyl chains. The compound, C60-fused *N*-methylpyrrolidine-*meta*-C12 phenyl (C60MC12), has actually been proved to exhibit high electron mobility [16].

The above results highlight the important role of molecular packing on charge transport of organic semiconductors. In other words, there is still room to improve the performance of OFETs by optimizing the molecular packing and/or the molecular orientation in the devices. In this paper, for evaluating the effect of alkyl-chain orientation, we have synthesized analogous compounds of C60MC12 and characterized their OTFT performances (Fig. 1). Using C_{60} derivatives with different alkyl-chain orientation, C60-fused *N*-methylpyrrolidine-*ortho*-C12 phenyl (C60OC12), C60MC12, C60-fused *N*-methylpyrrolidine-*para*-

* Corresponding authors. Tel.: +81 29 861 6252; fax: +81 29 861 6303.
E-mail addresses: m-chikamatsu@aist.go.jp (M. Chikamatsu), reiko.azumi@aist.go.jp (R. Azumi).

1010-6030/$ – see front matter © 2006 Elsevier B.V. All rights reserved.
doi:10.1016/j.jphotochem.2006.06.009

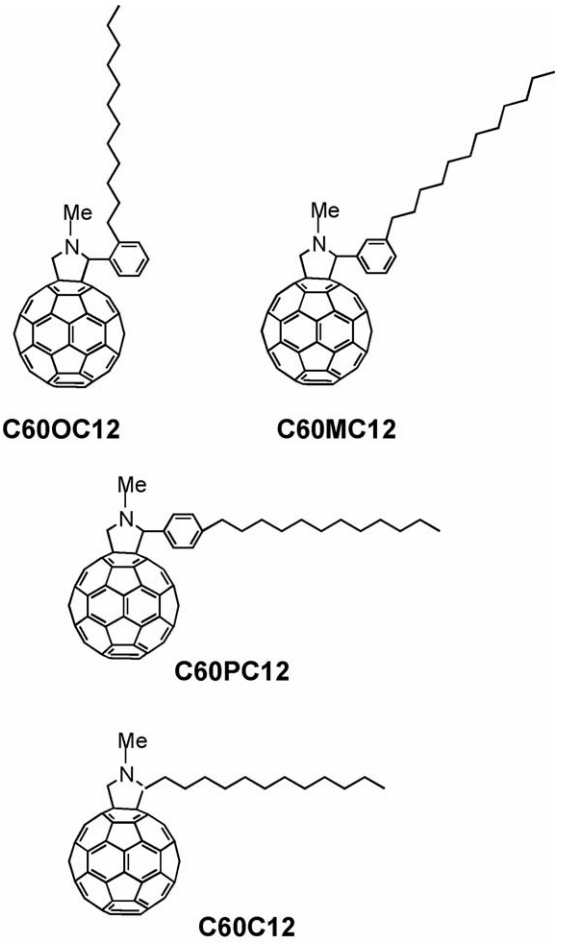

Fig. 1. Molecular structures of dodecyl-substituted C_{60} derivatives.

C12 phenyl (C60PC12) and C60-fused *N*-methylpyrrolidine-C12 (C60C12), we discuss the correlation between the film structures and TFT performance.

2. Experimental

2.1. General

^{1}H NMR spectra were recorded on a JEOL JNM-LA400 spectrometer, and chemical shift values were given in parts per million (ppm) relative to internal tetramethylsilane. Elemental analyses were performed on a CE INSTRUMENTS EA1110. Fast atom bombardment mass spectra (FAB-MS) were recorded on a JEOL MS 600H spectrometer using 3-nitrobenzylalcohol as a matrix.

2.2. Syntheses

C60OC12, C60MC12 and C60PC12 were synthesized via a similar route to the previous report [19,20].

C60C12: A mixture of *N*-methylglycine (53.4 mg, 0.6 mmol), tridecyl aldehyde (118.8 mg, 0.6 mmol) and C_{60} (432 mg, 0.6 mmol) was refluxed in toluene (800 mL) under N_2 atmosphere for 16 h. The clude product was separated by high-performance liquid chromatography. After vacuum evaporation of the solvent, C60C12 was obtained as a brown solid in 28% yield (160 mg, 0.17 mmol).

^{1}H NMR (400 MHz, $CDCl_3/CS_2$) δ 0.86 (t, $J = 6.0$ Hz, 3H, $(CH_2)_{11}CH_3$), 1.2–1.5 (m, 18H, $CH_2CH_2(CH_2)_9CH_3$), 1.86 (m, 2H, $CH_2CH_2(CH_2)_9CH_3$), 2.31 (m, 1H, one of $CH_2(CH_2)_{10}CH_3$), 2.44 (m, 1H, one of $CH_2(CH_2)_{10}CH_3$), 2.93 (s, 3H, NCH_3), 3.85 (t, $J = 5.4$ Hz, 1H, $NCHC_{60}$), 4.11 (d, $J = 9.6$ Hz, 1H, one of NCH_2C_{60}), 4.73 (d, $J = 8.8$ Hz, 1H, one of NCH_2C_{60}). Anal. calc. for $C_{75}H_{31}N$: C, 95.22; H, 3.30; N, 1.48. found: C, 94.55; H, 3.13; N, 1.38%. MS (FAB) *m/z* 946 ($M^+ + 1$).

2.3. Device fabrication and measurements

The devices were constructed on a highly doped p-type silicon wafer covered with 300-nm thick SiO_2 (a capacitance per unit area of 10 nF/cm^2). The SiO_2 surface was treated with hexamethyldisilazane (HMDS). Each film of C_{60} derivatives

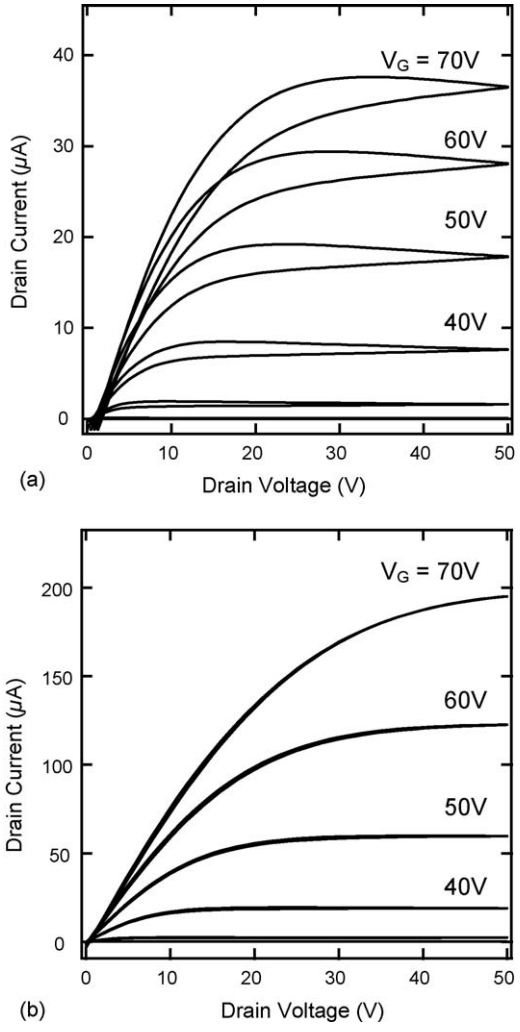

Fig. 2. (a) I_D–V_D characteristics of C60MC12-TFT before annealing. (b) I_D–V_D characteristics of C60MC12-TFT after annealing at 373 K for 12 h. The measurement was performed at 293 K.

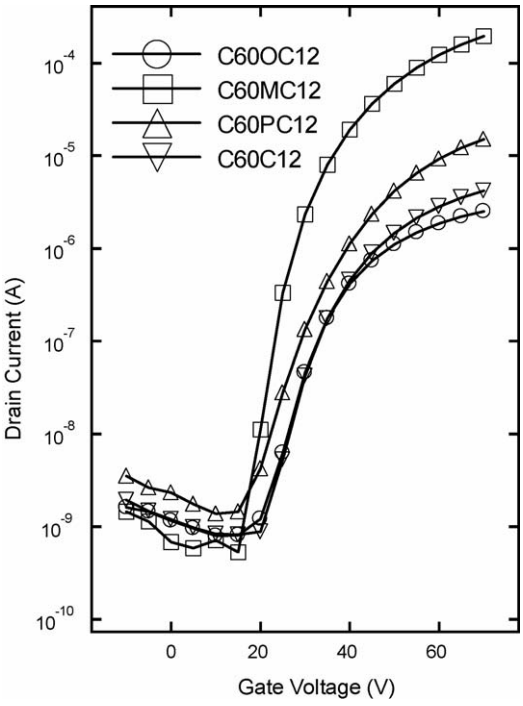

Fig. 3. I_D–V_G plots of the TFTs (V_D = 50 V, 293 K).

was fabricated on the SiO_2 layer by spin coating from 10 mg/ml chloroform solution under ambient condition. Spin-coating was performed at 500 rpm for 5 s, then at 2000 rpm for 60 s. Finally, gold source and drain electrodes were deposited on the films by using a resistive heating evaporation source. A nickel thin-plate patterned with channel lengths (L) of 20 μm and channel widths (W) of 5 mm was used as a metal shadow mask. For the measurement of the TFT characteristics, Au wires were connected to the device electrodes using silver paste. The TFT characteristics were measured with Keithley 6430 and 2400 source measurement units in vacuum (10^{-6} to 10^{-7} Torr).

2.4. Structural characterization of the spin-coated films

X-ray diffraction (XRD) measurement of the spin-coated films was carried out on a Rigaku Denki RU-300 using Cu Kα radiation (40 kV, 200 mA) with a curved graphite monochromator. The diffractions were measured from 2° to 25° in the 2θ–θ scan mode with 0.01°-step in 2θ and 0.6 s/step. An atomic force microscope (AFM, Molecular Imaging Inc. MS300) operating in contact mode was used to characterize the surface morphologies of the spin-coated films.

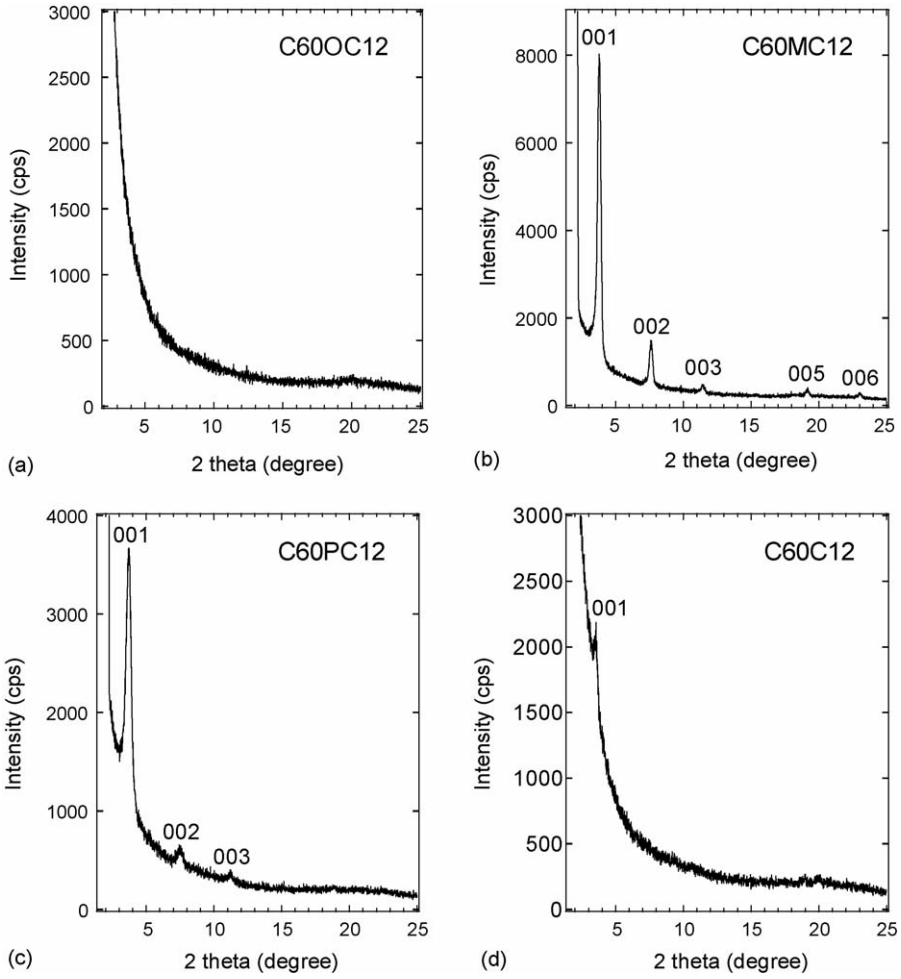

Fig. 4. XRD patterns of spin-coated C60OC12 (a), C60MC12 (b), C60PC12 (c) and C60C12 (d) films.

3. Results and discussion

3.1. Device characteristics

Fig. 2a shows drain current–drain voltage (I_D–V_D) characteristics of C60MC12-TFT at room temperature (293 K). The device showed *n*-channel characteristics with hysteresis in I_D curves. Fig. 2b shows the I_D–V_D characteristics of the same C60MC12-TFT device after annealed at 373 K for 12 h in vacuum. By the annealing I_D increased up to 195 μA at $V_D = 50$ V, $V_G = 70$ V, i.e., about 5-times higher than that of the non-annealed device (36 μA). In addition, hysteresis in I_D curves disappeared. In the case of the C60OC12-, C60PC12- and C60C12-TFTs, the values of I_D were also enhanced after the annealing. Hysteresis in I_D curves also diminished. We consider that the enhancement of I_D and the suppression of hysteresis by annealing are attributed to the improvement of molecular order and removal of oxygen gas, water and organic solvent that can act as trap species, disturbing electron transport.

Fig. 3 shows the drain current–gate voltage (I_D–V_G) plots of the TFTs at $V_D = 50$ V. The I_D values depend on the dodecyl-chain orientation of the C_{60} derivatives and range over two orders of magnitude. The C60MC12-TFT exhibites the highest value of I_D in the TFTs. The field-effect mobility μ and the threshold voltage V_T were estimated from the square root of drain current–gate voltage ($I_D{}^{1/2}$–V_G) plots, according to the standard equation in the saturation regime [1], $I_D = (W/2L)\mu C_i(V_G - V_T)^2$, where I_D is the drain current, W and L are the conduction channel width and length, respectively, C_i the capacitance per unit area of gate dielectric, V_G the gate voltage.

Table 1
Field-effect mobilities (μ), threshold voltages (V_T) and on/off current ratios (I_{on}/I_{off}) of dodecyl-substituted C_{60} derivatives

	μ (cm^2/Vs)	V_T (V)	I_{on}/I_{off}
C60OC12	1.5×10^{-3}	25.1	3×10^3
C60MC12	9.0×10^{-2}	27.0	4×10^5
C60PC12	8.1×10^{-3}	29.7	1×10^4
C60C12	2.2×10^{-3}	27.1	5×10^3

The field-effect electron mobility, threshold voltages and on/off current ratios (I_{on}/I_{off}) of TFTs are summarized in Table 1. All TFTs showed high electron mobitilies larger than 10^{-3} cm^2/Vs. The field-effect mobility is in the order of C60MC12 ≫ C60PC12 > C60C12 ∼ C60OC12. The C60MC12-TFT exhibited the highest mobility of 0.09 cm^2/Vs and I_{on}/I_{off} of 4×10^5. The mobility value is higher than that of n-type polymer, poly(benzobisimidazobenzophenanthroline), -TFTs in the saturation regime (0.03–0.05 cm^2/Vs) [13].

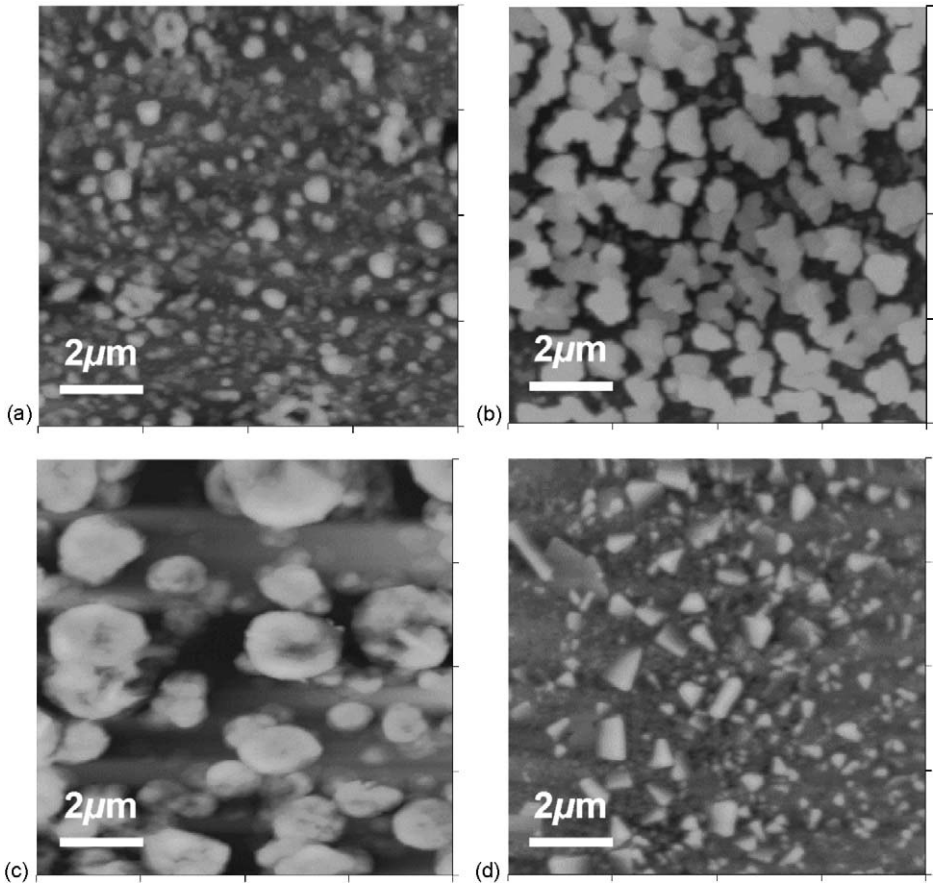

Fig. 5. AFM images of spin-coated C60OC12 (a), C60MC12 (b), C60PC12 (c) and C60C12 (d) films.

3.2. Film structure

After the TFT measurement, the C_{60} derivative films were subjected to out-of-plane XRD measurements and AFM observations. Film crystallinity and morphology are quite different among the four compounds. In the case of the C60MC12 and C60PC12 films, 00*l* reflections were observed up to higher-order and no other reflections were observed below 25° in 2θ (Fig. 4b and c). These results indicate that the C60MC12 and C60PC12 films take a well-ordered layer structure, that is, the crystallites are preferentially oriented with the (0 0 1) plane parallel to the substrate. The AFM images demonstrate that the C60MC12 and C60PC12 films consist of large grains of the size >1 μm (Fig. 5b and c). On the contrary, no sharp diffraction peaks were observed in the C60OC12 or C60C12 films from the XRD measurements (Fig. 4a and d). The AFM images also demonstrate that the C60OC12 and C60C12 films consist of small grains (Fig. 5a and d). The above results indicate the order of the film crystallinity as C60MC12 > C60PC12 ≫ C60C12 > C60OC12, which agrees with the order of mobilities: C60MC12 (9.0×10^{-2} cm^2/Vs), C60PC12 (8.1×10^{-3} cm^2/Vs), C60C12 (2.2×10^{-3} cm^2/Vs) and C60OC12 (1.5×10^{-3} cm^2/Vs).

The spacings of the (0 0 1) plane of the C60MC12, C60PC12 and C60C12 films calculated by Bragg's equation are 2.33 nm, 2.37 nm and 2.48 nm, respectively. The XRD peak patterns and the d-spacings of C60MC12 and C60PC12 spin-coated films agree with those of the previously reported cast films [19]. We also characterized in-plane structure of the C60MC12 and C60PC12 cast films by using grazing incidence X-ray diffraction (GIXD) measurements. The results indicated that C_{60} moieties form two-dimensional arrangement of the square lattice ($a = 10.1$ Å, $\gamma = 90°$). Since the diameter of C_{60} is 10.0 Å in a closed-packed single crystal [21], it is considered that π–π intermolecular overlap between C_{60} moieties is strong in the C60MC12 and C60PC12 films. High electron mobilities of the TFTs are considered to be due to the smooth electron conduction in crystalline domain with ordered C_{60} layer.

4. Conclusions

We have fabricated and characterized OTFTs based on various dodecyl-substituted C_{60} derivatives. We have found that not only chain-length but also chain-orientation play an important role for fabrication of highly ordered crystalline film, then leading to high electron mobility in solution-processed n-type OTFTs. C60MC12 exhibits excellent field-effect performance, with an electron mobility as high as 0.09 cm^2/Vs and current on/off ratio of up to 4×10^5. Our results have demonstrated the importance of molecular order in the film, and have shown the possibility of further improvement of the OTFT performance.

Acknowledgement

We thank Mr. J. Chisaka for his assistance with the atomic force microscopic measurements.

References

[1] C.D. Dimitrakopoulos, P.R.L. Malenfant, Adv. Mater. 14 (2002) 99.
[2] H. Sirringhaus, Adv. Mater. 17 (2005) 2411.
[3] H. Sirringhaus, P.J. Brown, R.H. Friend, M.M. Nielsen, K. Bechgaard, B.M.W. Langeveld-Voss, A.J.H. Spiering, R.A.J. Janssen, E.W. Meijer, P. Herwig, D.M. de Leeuw, Nature 401 (1999) 685.
[4] B.S. Ong, Y. Wu, P. Liu, S. Gardner, J. Am. Chem. Soc. 126 (2004) 3378.
[5] J.-F. Chang, B. Sun, D.W. Breiby, M.M. Nielsen, T.I. Sölling, M. Giles, I. McCulloch, H. Sirringhaus, Chem. Mater. 16 (2004) 4772.
[6] M. Heeney, C. Bailey, K. Genevicius, M. Shkunov, D. Sparrowe, S. Tierney, I. McCulloch, J. Am. Chem. Soc. 127 (2005) 1078.
[7] H.E. Katz, J.G. Laquindanum, A.J. Lovinger, Chem. Mater. 10 (1998) 633.
[8] A.R. Murphy, J.M.J. Fréchet, P. Chang, J. Lee, V. Subramanian, J. Am. Chem. Soc. 126 (2004) 1596.
[9] P.T. Herwig, K. Müllen, Adv. Mater. 11 (1999) 480.
[10] A. Afzali, C.D. Dimitrakopoulos, T.L. Breen, J. Am. Chem. Soc. 124 (2002) 8812.
[11] T. Minakata, Y. Natsume, Synth. Met. 153 (2005) 1.
[12] M.M. Payne, S.R. Parkin, J.E. Anthony, C.-C. Kuo, T.N. Jackson, J. Am. Chem. Soc. 127 (2005) 4986.
[13] A. Babel, S.A. Jenekhe, J. Am. Chem. Soc. 125 (2003) 13656.
[14] T.D. Anthopoulos, C. Tanase, S. Setayesh, E.J. Meijer, J.C. Hummelen, P.W.M. Blom, D.M. de Leeuw, Adv. Mater. 16 (2004) 2174.
[15] T.-W. Lee, Y. Byun, B.-W. Koo, I.-N. Kang, Y.-Y. Lyu, C.H. Lee, L. Pu, S.Y. Lee, Adv. Mater. 17 (2005) 2180.
[16] M. Chikamatsu, S. Nagamatsu, Y. Yoshida, K. Saito, K. Yase, K. Kikuchi, Appl. Phys. Lett. 87 (2005) 203504.
[17] X. Yang, J.K.J. van Duren, M.T. Rispens, J.C. Hummelen, R.A.J. Janssen, M.A.J. Michels, J. Loos, Adv. Mater. 16 (2004) 802.
[18] M. Chikamatsu, T. Hanada, Y. Yoshida, N. Tanigaki, K. Yase, H. Nishikawa, T. Kodama, I. Ikemoto, K. Kikuchi, Mol. Cryst. Liq. Cryst. 316 (1998) 157.
[19] M. Chikamatsu, K. Kikuchi, T. Kodama, H. Nishikawa, I. Ikemoto, N. Yoshimoto, T. Hanada, Y. Yoshida, N. Tanigaki, K. Yase, Nanonetwork Mater.: Am. Inst. Phys. Conf. Proc. 590 (2001) 455.
[20] X. Shi, W.B. Caldwell, K. Chen, C.A. Mirkin, J. Am. Chem. Soc. 116 (1994) 11598.
[21] W. Krätschmer, L.D. Lamb, K. Fostiropoulos, D.R. Huffman, Nature 347 (1990) 354.